

## HOMOLOGY MODELING AND *IN SILICO* DOCKING ANALYSIS OF HUMAN MITOCHONDRIAL THYMIDINE KINASE 2 USING GRID-BASED LIGAND DOCKING WITH ENERGETICS

RADHA MAHENDRAN\*, SUGANYA JEYABASKER, SHARANYA MANOHARAN, ANBARASU KRISHNAN, ASTRAL FRANCIS

Department of Bioinformatics, School of Life Sciences, Vels University, Chennai, Tamil Nadu, India.

Email: mahenradha@gmail.com/hodbioinfo@velsuniv.ac.in

Received: 19 January 2017, Revised and Accepted: 08 February 2017

### ABSTRACT

**Objective:** Mitochondrial disorders linked to thymidine kinase 2 (TK2) deficiency are associated with long-term treatment with antiviral nucleoside analogs such as azidothymidine (AZT). The accumulation of AZT-triphosphate affects deoxyribonucleic acid (DNA) polymerase, resulting in mitochondrial DNA depletion. Thus, a potent and selective inhibitor for TK2 is essential to be predicted.

**Methods:** The human mitochondrial TK2 was modeled using a modeler, and the structure was evaluated using Ramachandran Plot. The ligand molecule of both the derivatives of deoxythymidine (dThd) and thiourea was optimized using ChemSketch and was further docked using grid-based ligand docking with energetics Schrödinger package 2009.

**Results:** The human mitochondrial TK2 was modeled and the structure was validated using Procheck which had 90.1% of residues in the most favorable regions and 8.8% of residues in the allowed regions with 8 glycine residues and 10 proline residues. Docking analysis was carried out against the ligands selected from the dThd and thiourea derivatives, out of which 6, 8F, 8G, 8H, and 14B ligands had significant interacting poses with target protein TK2. In Ligand 6, the best interaction is found to be at 163 Glu molecule with a distance of 2.8 Å; in Ligand 8F, 172 Tyr, 63 Tyr, and 164 Glu with a distance of 2.8 Å; in Ligand 8G, 74 Gln with a distance of 2.7 Å, and in Ligand 14B, 107 Phe with a distance of 2.9 Å. From this, the dThd analog (Ligand 14B) could be a potent and selective inhibitor of TK2.

**Conclusion:** The present study indicated that dThd derivatives interacted significantly and hence serve as selective inhibitors against human mitochondrial TK2.

**Keywords:** Thymidine kinase 2, Azidothymidine-triPhosphate, Docking, Grid-based ligand docking with energetics, Deoxythymidine, Thiourea.

© 2017 The Authors. Published by Innovare Academic Sciences Pvt Ltd. This is an open access article under the CC BY license (<http://creativecommons.org/licenses/by/4.0/>) DOI: <http://dx.doi.org/10.22159/ajpcr.2017.v10i5.17185>

### INTRODUCTION

In mammalian cells, there are two deoxyribonucleoside kinases that can phosphorylate thymidine, namely cytosolic thymidine kinase (TK1) and mitochondrial TK2 [1]. TK2, encoded on chromosome 16q22 of the human genome, was a deoxynucleoside kinase that catalyzes the phosphorylation of the pyrimidine deoxynucleosides 2'-deoxythymidine (dThd), 2'-deoxyuridine (dUrd), and 2'-deoxycytidine (dCyd) to the corresponding deoxynucleoside 5'-monophosphate derivatives [2]. Deficiency in TK2 activity due to genetic alterations causes devastating mitochondrial diseases, which were characterized by mitochondrial deoxyribonucleic acid (mtDNA) depletion or multiple deletions in the affected tissues [3]. Deoxyribonucleoside kinases phosphorylate deoxyribonucleosides, a crucial reaction in biosynthesis of DNA precursors through the salvage pathway. Both TKs show important differences in their primary amino acid sequences, substrate specificities, and levels of expression in the different phases of the cell cycle [4]. The amino acid sequence of the TK1 enzymes was unique in its group whereas TK2 belongs to a larger group of nucleosides. AZT was an excellent substrate for TK1 and it was a poor substrate for TK2 [5]. Two of the four human deoxyribonucleoside kinases, deoxyguanosine kinase and TK2, were expressed in mitochondria. Human diacylglycerol kinases efficiently phosphorylate deoxyguanosine and deoxyadenosine, whereas TK2 phosphorylates dThd, dCyd, and dUrd. Mutations in TK2 represent a new etiology for mitochondrial DNA depletion, underscoring the importance of the mitochondrial deoxyribonucleotide (dNTP) pool in the pathogenesis of mitochondrial depletion [6]. The accumulation of AZT-TP was suggested to affect DNA polymerase resulting in mtDNA depletion [7,8]. DNA polymerase- $\gamma$  (pol- $\gamma$ ) was part of an assembly of

proteins and enzymes responsible for the replication of mtDNA. AZT-TP is one of the analogs least likely to be incorporated into DNA by DNA pol- $\gamma$ , but once AZT-MP is incorporated, it is not efficiently removed from DNA by the DNA pol- $\gamma$  exonuclease function [4,9].

### METHODS

#### Homology modeling

The protein sequence of human mitochondrial TK2 was obtained from the NCBI (<http://www.ncbi.nlm.nih.gov/>). BLASTP was used to identify the most suitable template based on sequence identity and score for homology modeling of human mitochondrial TK2. The available structure was *Drosophila melanogaster* nucleoside (PDB ID: 10T3) and was used as template. The homology modeling was carried out using Modeller 9V7 (Fig. 1). Modeller is a computer program that models three-dimensional (3D) structure of proteins and their assemblies by satisfaction of spatial restraints. The core modeling procedure begins with an alignment of the sequence to be modeled (target) with related known 3D structure (template). Then, the spatial features, such as C $\alpha$ -C $\alpha$  distance, hydrogen bonds, and main chain and side chain dihedral angles, are transferred from the templates to the target [10].

#### Structure validation

The structure verification program PROCHECK was used to evaluate the quality of the modeled 3D structure of mitochondrial TK2. The above-mentioned validation program validates the predicted structure by checking various parameters. PROCHECK, a structure verification program relies on Ramachandran plot (Fig. 2), determines the quality of the predicted structure by assessing various parameters such as

lengths, angles, and planarity of the peptide bonds, geometry of the hydrogen bonds, and side chain conformations of protein structures as a function of atomic resolution [10,11].

#### Protein preparation

The protein preparation consists of two components, preparation and refinement. After ensuring chemical correctness, the preparation

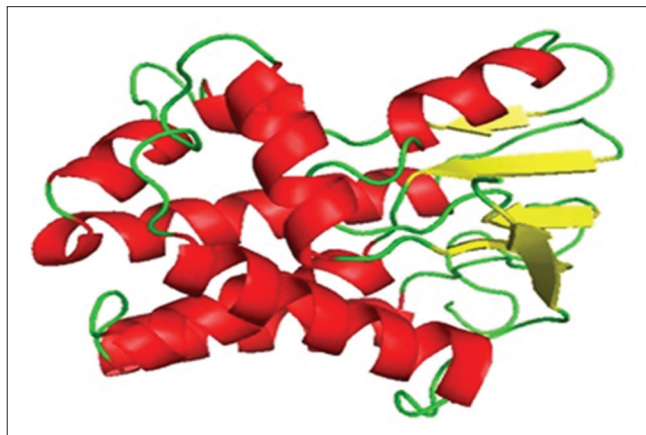


Fig. 1: Modeled structure of human mitochondrial thymidine kinase 2 using *Drosophila melanogaster* nucleoside as template (PDB ID: 10T3)

component adds hydrogen and neutralizes side chains that were not close to the binding cavity and did not participate in salt bridges. The refinement component performs a restrained impact minimization of the co-crystallized complex, which reorients side chain hydroxyl groups and alleviates potential steric clashes.

#### Ligand preparation

All the ligand structures (dThd/thiourea analogs) were taken from literature (Table 1). Ligand structures were drawn using ChemSketch. ACD/ChemSketch is the powerful chemical drawing and graphics package from ACD/labs software, which will draw molecular structures, reactions, and calculate chemical properties very quickly and easily [12]. The crystal structure was then refined, and the geometries were optimized with the OPLS-2005 force field using standard protocol and parameters [13].

#### Molecular docking

Molecular docking is the formation of non-covalent protein-ligand complexes in drug design. In the specified structure of a protein and a ligand, the task is predicting the structure of the binder complex. A docking technique evaluates the forces involved in the protein-ligand recognition such as Van der Waals bonding through hydrogen, electrostatic and place of the ligand appropriately in the active site [14]. These studies were done using grid-based ligand docking with energetics (GLIDE), and the crystal structure was cleaned by deleting the ligand and the cofactors. This was followed by adding hydrogen atoms in their standard geometry, adjusting the bond orders and formal charges. The crystal structure was then refined, and the geometries were optimized [13].

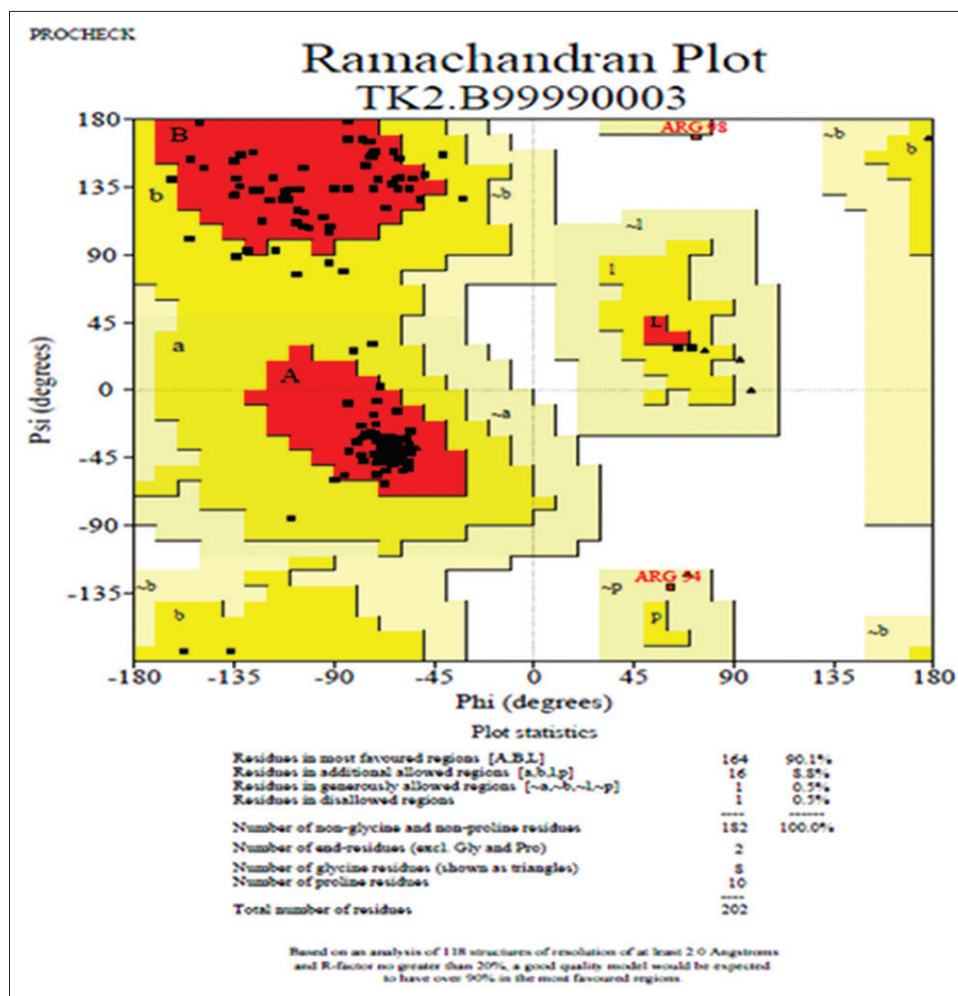
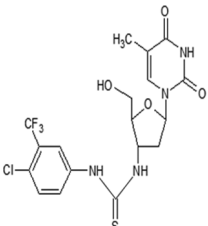
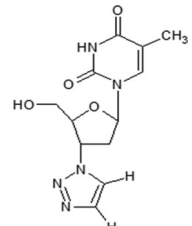
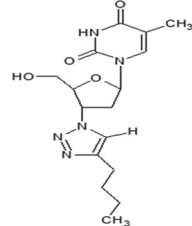
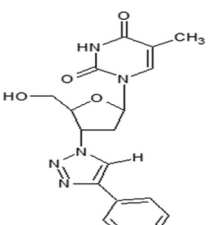
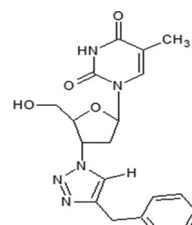
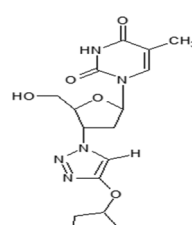
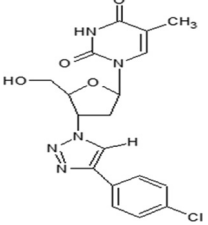
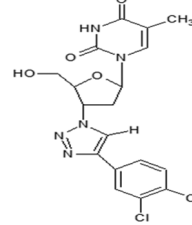
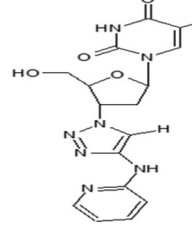
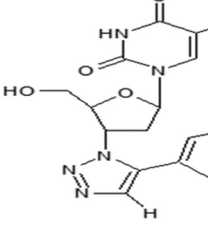
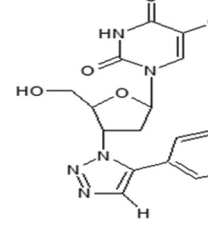
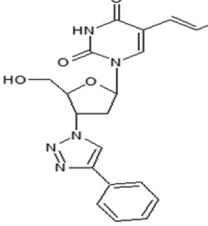
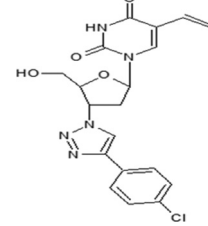


Fig. 2: Ramachandran plot for the modeled protein structure

Table 1: dThd and thiourea analogues used for Induced fit docking with IC<sub>50</sub> (μM)

<p>Ligand 6</p>  <p>Formula: C<sub>18</sub>H<sub>7</sub>ClN<sub>5</sub>O<sub>4</sub>SF<sub>3</sub> IC<sub>50</sub> (μM): 0.15±0.01</p>	<p>Ligand 8a</p>  <p>Formula: C<sub>12</sub>H<sub>7</sub>N<sub>5</sub>O<sub>4</sub> IC<sub>50</sub> (μM): 4.7±2.1</p>	<p>Ligand 8b</p>  <p>Formula: C<sub>16</sub>H<sub>9</sub>N<sub>5</sub>O<sub>3</sub> IC<sub>50</sub> (μM): 0.23±0.05</p>
<p>Ligand 8c</p>  <p>Formula: C<sub>18</sub>H<sub>6</sub>N<sub>5</sub>O<sub>4</sub> IC<sub>50</sub> (μM): 0.32±0.01</p>	<p>Ligand 8d</p>  <p>Formula: C<sub>19</sub>H<sub>6</sub>N<sub>5</sub>O<sub>4</sub> IC<sub>50</sub> (μM): 0.30±0.12</p>	<p>Ligand 8e</p>  <p>Formula: C<sub>17</sub>H<sub>6</sub>N<sub>5</sub>O<sub>5</sub> IC<sub>50</sub> (μM): 0.15±0.02</p>
<p>Ligand 8f</p>  <p>Formula: C<sub>18</sub>H<sub>6</sub>ClN<sub>5</sub>O<sub>4</sub> IC<sub>50</sub> (μM): 0.046±0.002</p>	<p>Ligand 8g</p>  <p>Formula: C<sub>18</sub>H<sub>6</sub>Cl<sub>2</sub>N<sub>5</sub>O<sub>4</sub> IC<sub>50</sub> (μM): 0.042±0.008</p>	<p>Ligand 8h</p>  <p>Formula: C<sub>17</sub>H<sub>7</sub>N<sub>7</sub>O<sub>4</sub> IC<sub>50</sub> (μM): 1.3±0.4</p>
<p>Ligand 8i</p>  <p>Formula: C<sub>17</sub>H<sub>6</sub>N<sub>5</sub>O<sub>4</sub> IC<sub>50</sub> (μM): 1.1±0.6</p>	<p>Ligand 8j</p>  <p>Formula: C<sub>17</sub>H<sub>6</sub>ClN<sub>5</sub>O<sub>4</sub> IC<sub>50</sub> (μM): 4.0±0.0</p>	
<p>Ligand 14a</p>  <p>Formula: C<sub>17</sub>H<sub>6</sub>ClN<sub>5</sub>O<sub>4</sub> IC<sub>50</sub> (μM): 0.25±0.09</p>	<p>Ligand 14b</p>  <p>Formula: C<sub>17</sub>H<sub>6</sub>ClN<sub>5</sub>O<sub>4</sub> IC<sub>50</sub> (μM): 0.036±0.003</p>	

dThd: Deoxythymidine

### Docking analysis using Maestro

Maestro is a graphical user interface for all Schrödinger's products. It contains tools for building, displaying, and manipulating chemical structures; for organizing, loading, and storing these structures and associated data; and also setting up, monitoring, and visualizing the results of calculations on these structures [15].

### Grid generation

Choose receptor grid generation from the glide submenu of the applications menu. The receptor grid generation panel has three tabbed folders to specify settings for the receptor grid generation job.

- Receptor
- Site
- Constraints

### Specifying the receptor grid

To specify the receptor grid for the docking job, click browse in the receptor grid section of the settings folder to open a file selector and choose a grid file (.grd). The file name, without the .grd extension, is displayed in the Receptor grid base name text box. We can also enter the base name directly into the text box [16].

### Induced fit docking

Glide docking uses the assumption of a rigid receptor although scaling of Van der Waals radii of non-polar atoms decreases penalties for close contacts. The induced fit docking allows the receptor to alter its binding sites so that it more closely conforms to the shape and binding mode of the ligand. Docking of both dThd and thiourea derivatives is done against the target TK2. The best glide energy and dock score were seen for the ligands. The best ligands were chosen for induced fit docking. Schrödinger has developed a Python script that automates the induced fit docking process. This Python script has an interface in Maestro, in which one can specify the structures and enter settings for various options, and then run the job. The structures used for induced fit docking must be prepared in the same manner as for GLIDE [17,18].

## RESULTS AND DISCUSSION

The human mitochondrial TK2 protein was modeled and the structure was validated using PROCHECK.

The percentage of residues for the modeled protein that were present in the most favorable regions of Ramachandran plot is 90.1%, whereas in allowed regions (a, b, l, p), it corresponds to give 8.8%. The number of glycine and proline residues was 8 and 10, respectively.

The ligands of both dThd and thiourea derivatives were drawn in ChemSketch and were docked against the target protein using GLIDE. The results were shown in Table 2.

From the results obtained, upon induced fit docking of the selected ligands, only 6, 8F, 8G, 8H, and 14B had significant interacting poses with the target protein TK2. Among the several poses generated, only the pose of the first and best showing docking score/glide energy was represented in the present study (Table 3).

The ligands interacted with the modeled human mitochondrial TK2 protein by forming hydrogen bonds.

The hydrogen bond interaction between the ligand and the protein occurs through the following residues:

The Ligand 6 (thiourea derivative) had a dock score of -9.10 with a glide energy of -59.11 Kcal/mol and interacted with 51 Arg with a distance of 3.0 Å, 163 Glu with a distance of 2.8 Å, 165 Glu with a distance of 3.5 Å, 160 Arg with a distance of 3.1 Å, 165 Glu with a distance of 3.3 Å, 164 Glu with a distance of 3.2 Å, and 63 Tyr with a distance of 3.1 Å.

The Ligand 8F (dThd analogs) had a dock score of -8.29 with a glide energy of -59.49 Kcal/mol and interacted with 172 Tyr with a distance

**Table 2: Docking results of both dThd and thiourea derivatives against the target thymidine kinase**

Ligands	Dock score	Glide energy kcal/mol	D-H...A	(Distance Å)
8F	-8.28	-50.19	74 Gln N-H...O	2.8
			74 Gln N-H...O	3.3
8H	-7.38	-45.94	74 Gln N-H...O	3.2
			45 Glu N-H...O	3.0
8H	-6.86	-44.27	45 Glu N-H...O	3.0
			74 Gln N-H...O	3.2
8G	-6.70	-46.16	No interaction	
			45 Glu N-H...O	2.9
6	-6.59	-49.46	24 Ala N-H...O	3.2
			65 Glu O-H...O	2.7
14A	-6.58	-45.72	51 Arg N-H...O	2.8
			65 Glu O-H...O	2.7
14B	-5.97	-49.05	No interaction	
			24 Ala N-H...O	3.1
8D	-5.61	-29.52	No interaction	
			24 Ala N-H...O	3.1
8I	-5.37	-19.87	No interaction	
			98 Arg N-H...O	2.6
8J	-5.20	-37.68	No interaction	
			51 Arg N-H...O	3.1
8A	-5.05	-26.82	51 Arg N-H...O	3.1
			51 Arg N-H...O	3.1
8E	-4.93	-36.03	51 Arg N-H...O	3.1
			51 Arg N-H...O	3.3
8C	-4.60	-28.85	51 Arg N-H...O	3.3
			51 Arg N-H...O	3.0
8B	-4.51	-31.25	51 Arg N-H...O	3.0
			51 Arg N-H...O	3.0

TK2: Thymidine kinase 2, dThd: Deoxythymidine

of 2.8 Å, 63 Tyr with a distance of 2.8 Å, and 164 Glu with a distance of 2.8 Å.

The Ligand 8G (dThd analogs) had a dock score of -9.59 with a glide energy of -56.51 Kcal/mol and interacted with 172 Tyr with a distance of 2.9 Å, 74 Gln with a distance of 2.7 Å, and 98 Arg with a distance of 3.2 Å.

The Ligand 8H (dThd analogs) had a dock score of -9.78 with a glide energy of -57.06 Kcal/mol and interacted with 24 Ala with a distance of 3.3 Å, 27 Lys with a distance of 3.1 Å, 27 Lys with a distance of 3.1 Å, 98 Arg with a distance of 3.2 Å, and 74 Gln with a distance of 3.1 Å.

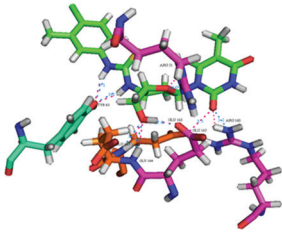
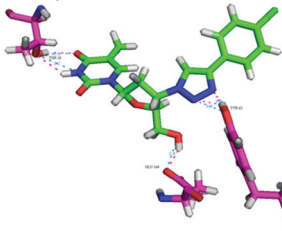
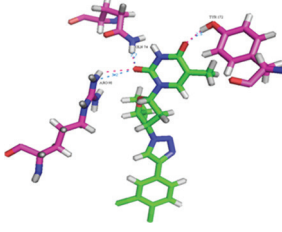
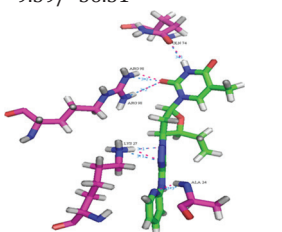
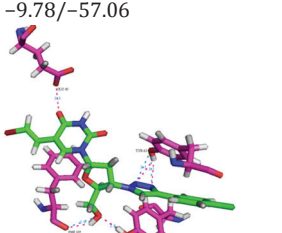
The Ligand 14B (bromovinyl derivative) had a dock score of -8.44 with a glide energy of -66.68 Kcal/mol and interacted with 45 Glu with a distance of 3.3 Å, 107 Phe with a distance of 2.9 Å, 172 Tyr with a distance of 2.8 Å, 63 Tyr with a distance of 3.2 Å, and 63 Tyr with a distance of 3.1 Å.

Mitochondrial DNA replication occurs throughout the whole cell cycle. This means that dNTPs are constantly required for mtDNA synthesis. If efficient targeting of TK2 inhibitors to the mitochondria becomes an achievable goal, it will become easier to investigate the role of TK2 in mitochondrial toxicity of antiviral and anticancer compounds, as well as other important issues such as mitochondrial homeostasis and integrity, the dynamics of mitochondrial dNTP pools, mitochondrial DNA repair, the possible existence of a substrate cycle between TK2 and mitochondrial nucleotidase(s), and the communication between mitochondria and the cytosol/nucleus [19]. In this study, dThd analogs and thiourea derivatives have been analyzed and Ligand 14B has been emerged as a selective inhibitor which could help in further analysis in reducing mtDNA depletion syndrome.

## CONCLUSION

The accumulation of AZT-TP was suggested to affect DNA polymerase resulting in mtDNA depletion syndrome. AZT-TP was formed as a result of phosphorylation of AZT by TK2. Hence, by inhibiting the action of TK2, phosphorylation of AZT could be controlled which automatically reduces the chances of mtDNA depletion syndrome. The earlier identified inhibitors of TK2 were of thiourea derivatives. By replacing the thiourea linker of an earlier identified TK2 inhibitor Ligand 6 by a 1, 4-substituted triazole ring (dThd analogs), a new generation of potent

Table 3: Induced fit docking results against the target TK2

Ligands	Interaction Docking score/glide energy (Kcal/mol)	D-H...A	Distance (Å)
6		51 Arg N-H...O 163 Glu O-H...O 165 Glu O-H...O 160 Arg N-H...O 165 Glu N-H...O 164 Glu N-H...O 63 Tyr N-H...O 63 Tyr N-H...O	3.0 2.8 3.5 3.1 3.3 3.2 3.1 3.1
8F	-9.10/-59.11 	172 Tyr O-H...O 63 Tyr O-H...O 164 Glu O-H...O	2.8 2.8 2.8
8G	-8.29/-59.49 	172 Tyr O-H...O 74 Gln N-H...O 98 Arg N-H...O	2.9 2.7 3.2
8H	-9.59/-56.51 	24 Ala N-H...N 27 Lys N-H...N 27 Lys N-H...N 98 Arg N-H...O 74 Gln N-H...O	3.3 3.1 3.1 3.2 3.1
14B	-9.78/-57.06 	45 Glu O-H...O 107 Phe O-H...O 172 Tyr O-H...O 63 Tyr O-H...N 63 Tyr O-H...N	3.3 2.9 2.8 3.2 3.1
	-8.44/-66.68		

TK2: Thymidine kinase 2

TK2 inhibitors was generated. Docking results showed that dThd analogs have good energy and comparable score as of Ligand 6. Ligand 14B has a best docking score (-9.05) and glide energy (-66.81) compared to the existing inhibitors of Ligand 6 which has score (-9.10) and energy (-59.11). Hydrogen bonding of Ligand 14B was also similar to that of thiourea derivative (Ligand 6). Hence, dThd analogs (Ligand 14B) have been emerged as potent and selective inhibitors of TK2.

#### REFERENCES

- Balzarini J, Zhu C, De Clercq E, Pérez-Pérez MJ, Chamorro C, Camarasa MJ, *et al.* Novel ribofuranosynucleoside lead compounds for potent and selective inhibitors of mitochondrial thymidine kinase-2. *Biochem J* 2000;351:167-71.
- Priego EM, Karlsson A, Gago F, Camarasa MJ, Balzarini J, Pérez-Pérez MJ. Recent advances in thymidine kinase 2 (TK2) inhibitors and new perspectives for potential applications. *Curr Pharm Des* 2012;18(20):2981-94.
- Sun R, Wang L. Thymidine kinase 2 enzyme kinetics elucidate the mechanism of thymidine-induced mitochondrial DNA depletion. *Biochemistry* 2014;53(39):6142-50.
- Eriksson S, Munch-Petersen B, Johansson K, Eklund H. Structure and function of cellular deoxyribonucleoside kinases. *Cell Mol Life Sci* 2002;59(8):1327-46.
- Al-Madhoun AS, Tjarks W, Eriksson S. The role of thymidine kinases in the activation of pyrimidine nucleoside analogues. *Mini Rev Med Chem* 2004;4(4):341-50.
- Saada A, Shaag A, Mandel H, Nevo Y, Eriksson S, Elpeleg O. Mutant

- mitochondrial thymidine kinase in mitochondrial DNA depletion myopathy. *Nat Genet* 2001;29(3):342-4.
7. Lewis W, Dalakas MC. Mitochondrial toxicity of antiviral drugs. *Nat Med* 1995;1(5):417-22.
  8. Lewis W, Day BJ, Copeland WC. Mitochondrial toxicity of NRTI antiviral drugs: An integrated cellular perspective. *Nat Rev Drug Discov* 2003;2(10):812-22.
  9. Chan SS, Copeland WC. DNA polymerase gamma and mitochondrial disease: Understanding the consequence of POLG mutations. *Biochim Biophys Acta* 2009;1787(5):312-9.
  10. Shrasti G, VijayLaxmi S, Brijendra S. Homology modeling and docking studies of neuraminidase protein of influenza A virus (H1N1) with select ligand - A computer aided structure based drug design. *Int J Pharm Sci Invent* 2013;2(6):35-41.
  11. John A, Umashankar V, Samdani A, Sangeetha M, Krishnakumar S, Deepa PR. *In silico* structure prediction of human fatty acid synthase-dehydratase: A plausible model for understanding active site interactions. *Bioinform Biol Insights* 2016;10:143-54.
  12. Manimekalai R, Victoriya MS, Shoba G. *In silico* docking analysis of carbazole alkaloids from *Murraya koenigii* against PP2A. *Int J Pharm Bio Sci* 2015;6(1):B913-28.
  13. Akshada J, Manoj G, Urmila JJ. Identification of potential novel EGFR inhibitors using a combination of pharmacophore and docking methods. *Int J Pharm Pharm Sci* 2015;7(6):???
  14. Jerad SA, Devi R, Noorulla KM, Surya PR. Insights into thioridazine for its anti-tubercular activity from molecular docking studies. *Int J Pharm Pharm Sci* 2015;7(3):???
  15. Dhurga K, Gunasekaran G, Senthilraja P, Manivel G, Stalin A. Molecular modeling and docking analysis of pseudomonas bacterial proteins with eugenol and its derivatives. *RJLBPCS* 2016;2(1):40.
  16. Jayaraman A, Jamil K, Kakarala KK. Homology modelling and docking studies of human  $\alpha$ 2-adrenergic receptor subtypes. *J Comput Sci Syst Biol* 2013;6:136-49.
  17. Hua-Jun L, Jun-Zhi W, Nian-Yu H, Wei-Qiao D, Kun Z. Induced-fit docking and virtual screening for 8-hydroxy-3-methoxy-5H-pyrido [2,1-c] pyrazin-5-one derivatives as inducible nitric oxide synthase inhibitors. *J Chem Pharm Res* 2014;6(3):1187-94.
  18. Vijayakumar B, Parasuraman S, Raveendran R, Velmurugan D. Identification of natural inhibitors against angiotensin I converting enzyme for cardiac safety using induced fit docking and MM-GBSA studies. *Pharmacogn Mag* 2014;10 Suppl 3:S639-44.
  19. Pérez-Pérez MJ, Hernández AI, Priego EM, Rodríguez-Barrios F, Gago F, Camarasa MJ, et al. Mitochondrial thymidine kinase inhibitors. *Curr Top Med Chem* 2005;5(13):1205-19.